

# Synthesis, structural and optical properties of ZnO thin films

N. Boussatha\*

Laboratoire d'Electrochimie, Corrosion, Métallurgie et  
Chimie Minérale. Faculté de Chimie USTHB. BP32 El-Alia  
Bab-Ezzouar.16111. Alger  
\*nadia-boussatha@live.fr

H. Ghoualem

Laboratoire d'Electrochimie, Corrosion, Métallurgie et  
Chimie Minérale. Faculté de Chimie USTHB. BP32 El-Alia  
Bab-Ezzouar.16111. Alger  
hghoualem@usthb.dz

**Abstract**—In this study we have investigated an economical route for the synthesis of ZnO thin films by sol-gel technique associated with spin-coating deposited onto silicon substrates post annealed at 550°C. Characterizations of the samples were performed by X-ray diffraction (XRD), Atomic Force Microscopy (AFM) and the diffuse reflectance of the films was measured using UV-VIS-NIR spectrophotometer. X-ray diffraction (XRD) of the films showed a hexagonal wurtzite-type structure with a preferential orientation according to the direction  $\langle 002 \rangle$ . Scherrer's formula was used to calculate crystallite size. AFM study revealed spherical uniform morphology of ZnO films. Finally, the various optical constants and the optical conductivity were measured.

**Keywords**—Oxidize zinc (ZnO), thin films, sol-gel, spin coating, optical properties. Force atomic microscopy.

## I. INTRODUCTION

Zinc oxide (ZnO) is a promising semiconductor material for use in blue/UV regions owing to its wide band gap (3.37 eV), a large exciton binding energy (60 meV) and a small Bohr radius (1.8 nm), which permits excitonic recombination even at room temperature [1]. In addition, it has chemical and thermal stability, high radiation resistance, high transparency, and good conductivity [2]. ZnO has attracted considerable attention due to its potential applications in solar cells [3], optoelectronic devices [4], thin film transistors (TFTs) [5], gas sensors [6,7], and photocatalysts [8], operating in UV range. ZnO thin films can be obtained by different methods such as spray pyrolysis [9], chemical vapour deposition [10], RF magnetron sputtering [11], pulsed laser deposition technique [12], etc. Sol-gel spin-coating has many advantages such as strong c-axis orientation, low cost, simplicity, safety, large area deposition feasibility, flexibility in the choice of substrates and the ability to control chemical composition. The sol-gel spin-coating method is therefore prevalent today and ideal for exploratory research.

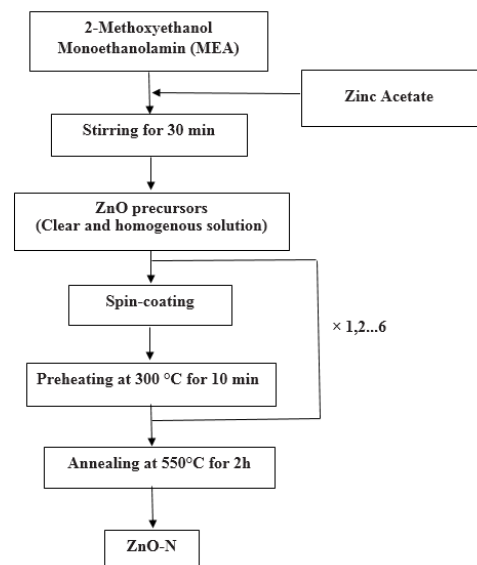
In this paper, we investigate a facile chemical preparation approach of zinc oxide very thin films with varied deposition cycles. Prepared samples were subjected to a series of microstructural characterizations. Optical properties are

investigated the UV-Visible spectral range and the results thus obtained were discussed.

## II. EXPERIMENTAL DETAILS

### A. Preparation of ZnO thin films

The ZnO precursor solution was obtained by dissolving zinc acetate dehydrate ( $\text{Zn}(\text{CH}_3\text{CO}_2)_2 \cdot 2\text{H}_2\text{O}$ ) in methoxyethanol ( $\text{C}_3\text{H}_8\text{O}_2$ ). Monoethanolamin ( $\text{C}_2\text{H}_7\text{NO}$ ) is used as a stabilizer. The mix is then stirred for 30 min at room temperature. The wafers were prepared by a standard cleaning procedure initially with ethanol, acetone and then distilled water, the solution is then deposited by spin-coating at a rotation speed of 2500 rpm for 30 s. The ZnO films are then subsequently pre-heated in a furnace at 300 °C for 10 min in order to evaporate the solvent residues. The deposition cycle, consisting in liquid deposition, spin-coating and preheating, is repeated up to 6 times to obtain layers with a gradually increased thickness. Three series of each sample have been elaborated to check the repeatability of the results. Finally, all samples were air-annealed at 550 °C for 2 h.



*B. Characterization methods*

The crystallinity of the ZnO films was studied by XRD method. The measurements were performed using Bruker D8-advance in the conventional  $\theta$ - $2\theta$  configuration. Surface morphology of the samples is characterized by an atomic force microscope (Digital instruments nanoscope III). Optical measurements were performed in order to obtain the optical band gap and other optical properties using a Jasco V-570 double beam spectrophotometer.

III. RESULTS AND DISCUSSION

*A. structural properties*

XRD measurements have been carried out on ZnO thin films in order to determine phase and crystallographic analysis. Fig. 1 shows the XRD patterns of ZnO thin films. Only the (0 0 2) diffraction peak was observed in the spectra, revealing a good orientation of the wurtzite structure of ZnO with c-axis perpendicular to the substrate plane.

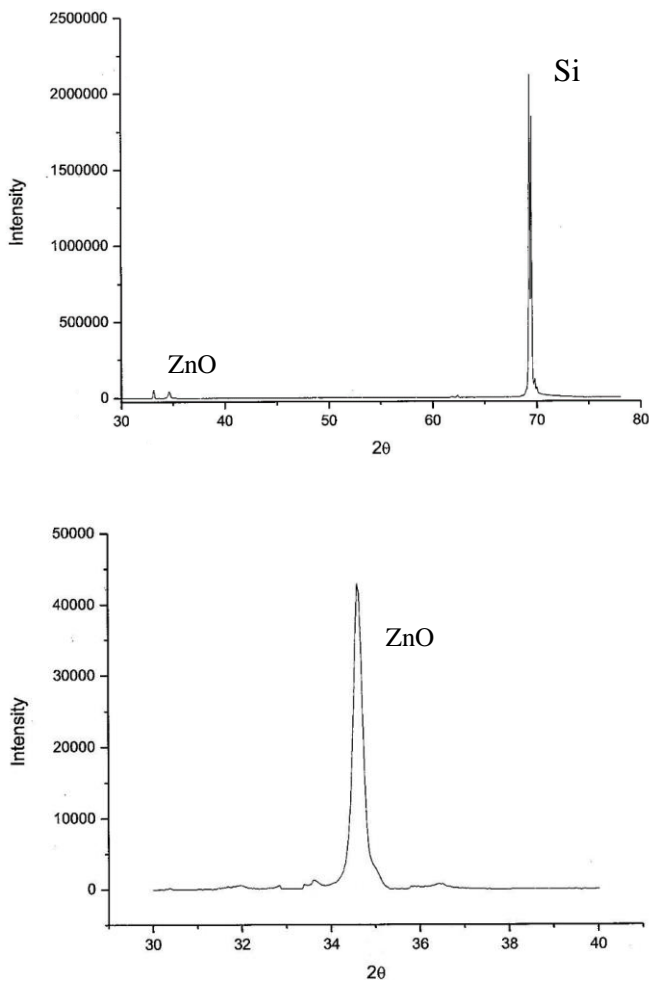


**Fig. 1** XRD spectrum of sol-gel spin-coated ZnO samples

*B. Morphological properties*

The surface morphologies of the samples have been observed by atomic force microscopy (AFM). AFM images are shown in Fig. 2 for 3 samples of 2, 4 and 6 deposition layers. The pictures reveal the formation of very small particles homogeneously distributed on the surface with some size distribution. It can be observed that for a given synthesis temperature and concentration, the size of the grains increases with number of deposited layers.

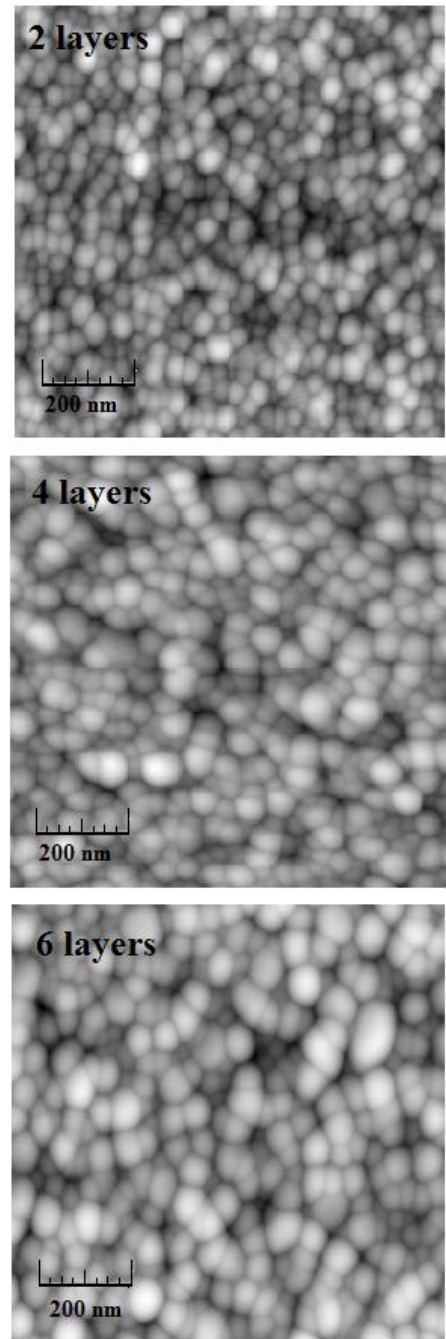


**Fig. 2** Atomic force microscopy micrographs ( $1\ \mu\text{m} \times 1\ \mu\text{m}$ ) of sol-gel spin-coated ZnO samples with 2, 4 and 6 deposited layers.

C. Optical properties

Optical reflectance measurements have been performed at room temperature, in a wavelength range from 200 to 11000 nm. The optical reflectance data have been used to estimate the band gap energy and the optical constants by employing a well-known analysis to determine absorption coefficient, extinction coefficient (k), optical conductivity ( $\sigma_{opt}$ ) and the refractive index (n).

Fig. 3 shows the UV-visible reflectance spectra of the synthesized films. The optical band gap ( $E_g$ ) is narrowly related (Tauc relationship) to absorption coefficient ( $\alpha$ ) and photon energy ( $h\nu$ ) (Eq. 1) [13].

$$(ah\nu) = A(h\nu - E_g)^n \dots\dots\dots (1)$$

n is equal to 1/2 for direct band gap,  $\alpha$  is the absorption coefficient estimated according to the Kubelka–Munk function,  $\alpha = F(R)/2R$ , and R the diffuse-reflectance [13]. Accordingly, the  $E_g$  values of ZnO samples were obtained from the linear intercept of the plots of  $(ah\nu)^2$  against photonenergy ( $h\nu$ ).

ZnO films exhibits a band gap of 2.88-3.16 eV, which is close to that reported in the literature. The results shown in Fig. 3 confirmed that the band gap increases slightly with the deposition cycles.

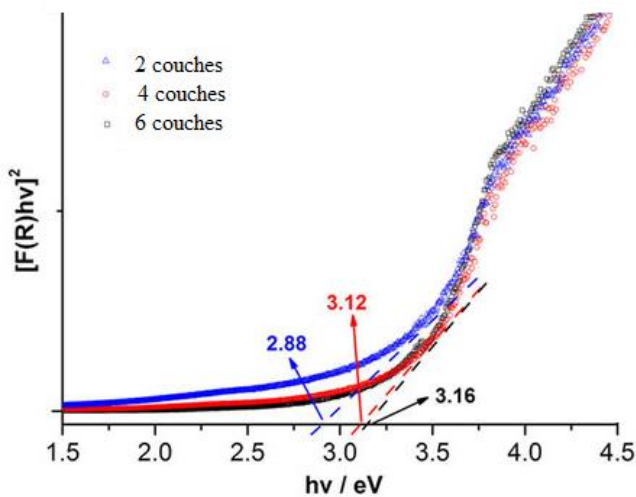


Fig. 3 Optical properties for ZnO thin films

The extinction coefficient k is evaluated with regard to the absorption coefficient ( $\alpha$ ) by [14]

$$k = \frac{\lambda\alpha}{4\pi} \dots\dots\dots (2)$$

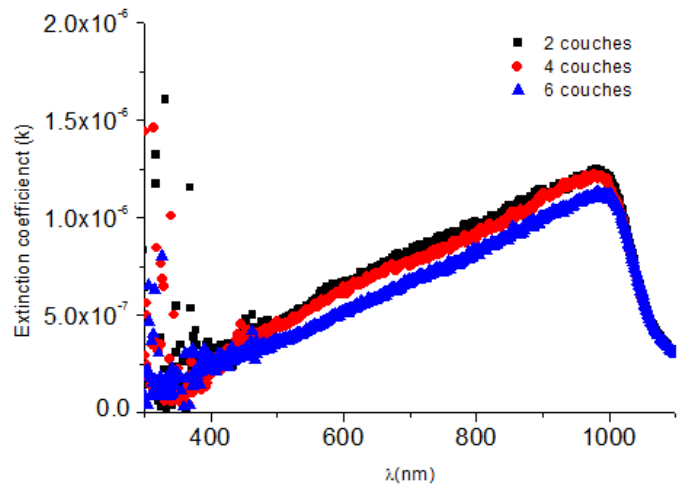


Fig. 4 Extinction coefficient against wavelength for ZnO thin films

Fig. 4 illustrates the evolution of the extinction coefficient k as a function of the wavelength. The curves reveal a strong expansion of the portion of light unexploited at ~ 980 nm. As the thickness of the films increases, the displacing of k's freefall point toward lower wavelengths, would result in a strong loss of the incident light by a diffusion mechanism.

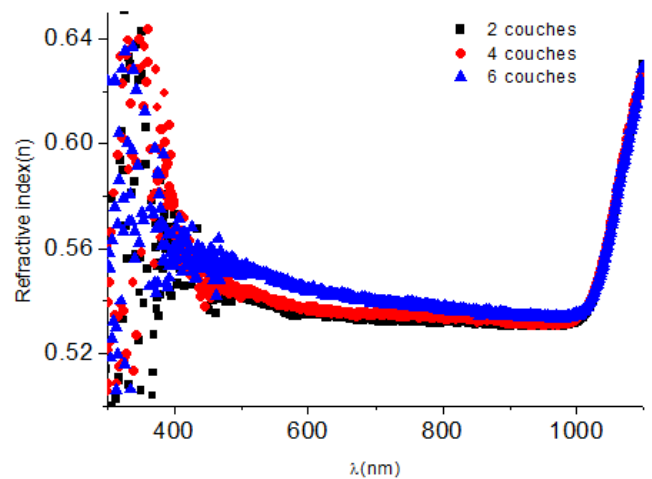


Fig. 5 Refractive index against wavelength for ZnO thin films

The interaction between the photons and electrons could be explained in terms of the variation of the refractive index (n) with the wavelength [14]. Using the reflectance data, the n index was estimated as follows [14]:

$$n = - \frac{(R + 1) \pm \sqrt{3R^2 + 10R - 3}}{2(R - 1)} \dots\dots\dots (3)$$

Fig. 5 shows the refractive index of the ZnO samples in the range of 300–1100 nm. The n index initially keeps constant with increasing the wavelength after which it increases above

1000 nm. Below that wavelength, the average refractive index of the grown crystals is 0.53. When  $n(\lambda)$  tends to be constant, that means that the material is nondispersive.

## References

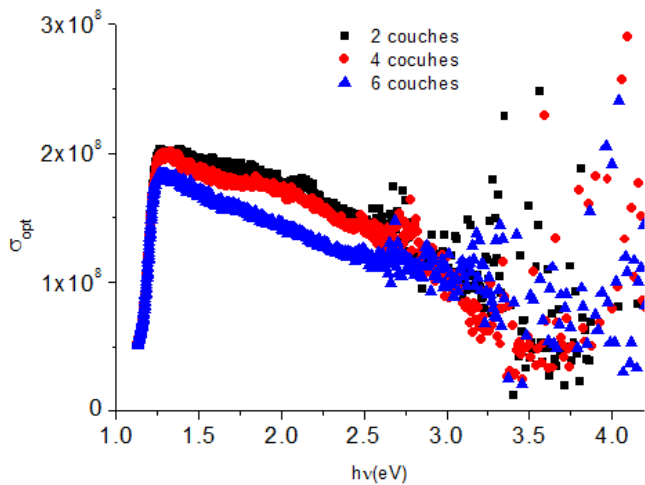


**Fig. 6** Optical conductivity against photonenergy for ZnO thin films

The optical conductivity ( $\sigma_{opt}$ ) of the elaborated films was assessed by [14].

$$\sigma_{opt} = \frac{\alpha n C}{4\pi} \dots \dots \dots (4)$$

**Fig. 6** illustrates  $\sigma_{opt}$  as a function of  $h\nu$ . For photon energy lower than  $\sim 1.27$  eV,  $\sigma_{opt}$  increases abruptly as the wavelength increases and a saturation of the optical conductivity is observed at 1.27 eV. However,  $\sigma_{opt}$  decreases when photon energy becomes higher than  $\sim 1.27$  eV.

## CONCLUSION

ZnO nanostructured layers have been elaborated using sol-gel and spin coating process yielding very thin layers. Thickness of the layers has been varied by varying the number of deposition cycles. A simultaneous evolution of grains morphology has been observed for the samples. This behaviour could be the consequence of a particular growth mechanism where the low thicknesses induces frustrated growth of grains and simultaneously prevents layers from making denser. It was observed that the thickness of the layers has a weak factor influencing the optical properties of ZnO films. The produced ZnO thin films revealed a good orientation of the wurtzite structure with a texture along the c-axis (002) of ZnO with c-axis perpendicular to the substrate plane. There are intrinsic correlations between the structural, optical and morphological properties of the ZnO thin films, which are crucial for future study and application of TCO and solar cells thin films.

- [1] R. Rajalakshmi, S. Angappane, Synthesis, characterization and photoresponse study of undoped and transition metal (Co, Ni, Mn) doped ZnO thin films, Mater. Sci. Eng. B 178 (2013) 1068–1075.
- [1] J. Ye, S. Gu, S. Zhu, T. Chen, L. Hu, F. Qin, R. Zhang, Y. Shi, Y. Zheng, The growth and annealing of single crystalline ZnO films by low-pressure MOCVD, J. Cryst. Growth 243 (2002) 151–156.
- [2] S. Kundu, U. Nithyanantham, DNA-mediated fast synthesis of shape-selective ZnO nanostructures and their potential applications in catalysis and dyesensitized solar cells, Ind. Eng. Chem. Res. 53 (2014) 13667–13679.
- [3] Ü. Özgür, Y.I. Alivov, C. Liu, A. Teke, M. Reshchikov, S. Doğan, V. Avrutin, S.J. Cho, H. Morkoc, J. Appl. Phys. 98 (2005) 041301.
- [4] M. Ortel, T. Balster, V. Wagner, Chemical composition and temperature dependent performance of ZnO-thin film
- [5] transistors deposited by pulsed and continuous spray pyrolysis, J. Appl. Phys. 114 (2013) 234502.
- [6] Q. Jia, H. Ji, Y. Zhang, Y. Chem, X. Sun, Z. Jin, J. Hazard. Mater. 276 (2014) 262.
- [7] J. Guo, J. Zhang, M. Zhu, D. Ju, H. Xu, B. Cao, Sens. Actuators B: Chem. 199 (2014) 339.
- [8] S. Kundu, A facile route for the formation of shape-selective ZnO nanoarchitectures with superior photo-catalytic activity, Colloids Surf., A 446 (2014) 199–212.
- [9] S. Sriram and A. Thayumanavan, Journal of electron devices 15, 1215–1224 (2012).
- [10] F. S. Sen Chien, C. R. Wang, Y. L. Chain and RJ Wu. Sensor Actuat Phys. B 144, 120–125 (2010).
- [11] Wang Xing-Hu, LI Rong-Bin and Fan Dong-Hua, Chin. Phys. Lett. 30, 037202 (2006).
- [12] M. Joseph, H. Tabata, H. Saeki, K. Ueda, T. Kawai Physica B, 302 (2001), pp. 140–148
- [13] A. Ayeshamariam, S. Ramalingam, M. Bououdina, M. Jayachandran, Spectrochim. Acta A: Mol. Biomol. Spectrosc. 118 (2014) 1135–1143, <http://dx.doi.org/10.1016/j.saa.2013.09.030>.
- [14] P.M. Dinakaran, S. Kalainathan, Optik 124 (2013) 5111–5115, <http://dx.doi.org/10.1016/j.ijleo.2013.03.073>.